A Simple Method to Account for Edge Shape in the Conductor Loss in Microstrip

Edward L. Barsotti, Edward F. Kuester, *Member, IEEE,* and John M. Dunn, *Member, IEEE*

Abstract —A new technique has been developed to examine the effect of strip edge shape on conductor loss in planar transmission lines using a modified incremental inductance rule. Based on Lewin's and Vainshtein's zero-thickness strip perturbation in loss calculations, this method requires an expression for the infinitely thin strip inductance, as well as prescribed integration *stopping points* for the different strip shapes. Results are given comparing loss for different edge shapes in a microstrip system, using both this new method and the Lewin/ Vainshtein technique. Finally, the differing results of some other published analytical and numerical loss methods based on the surface impedance boundary condition are compared.

I. INTRODUCTION

RECENTLY, Lewin [1] and Vainshtein [2] have independently developed a perturbation method of calculating the strip portion of the conductor loss of a nonzero-thickness microstrip using integrations of the currents from the limiting case of a quasi-TEM zero-thickness strip. The ground plane loss contribution is typically small in a microstrip environment, so the strip contribution forms the major part of the total conductor loss. In any event, the ground plane loss is more straightforward to compute, since no edges are involved, and we will regard it as readily calculated. The edge singularity in the loss integration is avoided in [1], [2] by stopping the integration just short of the edge by an amount determined by the local geometry near the nonzero-thickness edge. Division of the zero-thickness current into the portions on the top and bottom surfaces of the strip can be difficult in planar lines, particularly in microstrip. This new method allows comparison of the loss of planar transmission lines with different edge shapes from only a knowledge of the inductance of the corresponding structure with infinitely thin strips and also the integration stopping points. The technique is applicable to microstrip as well as other planar lines. Once accurate determination of the loss for a specific edge shape has been made from other methods, losses for strips with other edges can be found. The conductor loss in the specific case of a rectangular-edged microstrip is examined here in a survey of published analytical and numerical results [3]–[7] based on the surface impedance boundary condition. Finlay *et al.* [8] give results which are based on a modified

surface impedance condition, including the effects of the surface currents on both sides of the strip.

II. DERIVATION OF LOSS DIFFERENCE FORMULAS

A. Use of the Lewin/Vainshtein Current Integration Technique

For a highly conductive, nonzero-thickness strip, the assumption of a surface impedance boundary condition is often taken. Using $E_{\text{tan}} = Z_s a_n \times H_{\text{tan}}$, where $Z_s = (1 + j)R_s = (1 + j)\sqrt{\pi f \mu \rho}$ is the surface impedance and a_n the outward unit normal vector, and neglecting loss due to the ground plane, the loss integration can be reduced to the contour integral [3]

$$\alpha_c = \frac{R_s}{2Z_0} \oint_C \frac{|J_s|^2}{|I|^2} \, dl \tag{1}$$

where α_c is the attenuation constant in Np/m and C is the boundary of the nonzero-thickness strip cross section as in Fig. 1(a). Here Z_0 is the characteristic impedance of the transmission line, J_s is the z-directed surface current density on the longitudinally invariant ($\partial/\partial z = 0$) strip, and I is the total current of the strip. According to Lewin and Vainshtein, this contour integral can be replaced by a line integral using an infinitely thin, perfectly conducting strip with its correspondingly simpler longitudinal current distribution J_{z0}. Dividing this current into $J_{z0,\text{top}}$ and $J_{z0,\text{bot}}$, the top and bottom surface currents of the strip, respectively, the loss becomes

$$\alpha_c = \frac{R_s}{2Z_0 I^2} \int_{-w/2 + \Delta_l}^{w/2 - \Delta_r} \left[J_{z0,\text{top}}^2(x) + J_{z0,\text{bot}}^2(x) \right] dx \tag{2}$$

where Δ_l and Δ_r are the integration stopping points for the left and right edges, respectively (see Fig. 1(b)), and w is the strip width. Each stopping point, a very small distance from the edge singularity, is a function only of the local edge geometry, and is obtained by equating the loss in the zero-thickness case to the actual loss due to local nonzero edge effects under static approximations of the fields. The division of the ideal current expression J_{z0} into top and bottom strip currents $J_{z0,\text{top}}$ and $J_{z0,\text{bot}}$ is dependent on the planar transmission line configuration. As an example, the currents of the microstrip line of Fig. 2 will be separated by a Green's function technique.
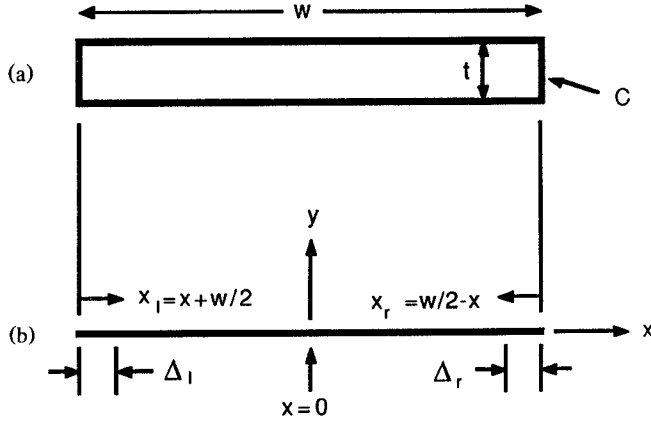
Fig. 1. (a) Finite-thickness strip with a rectangular edge. (b) Zero-thickness strip with integration stopping points Δ_l and Δ_r and Cartesian coordinates (x, y).
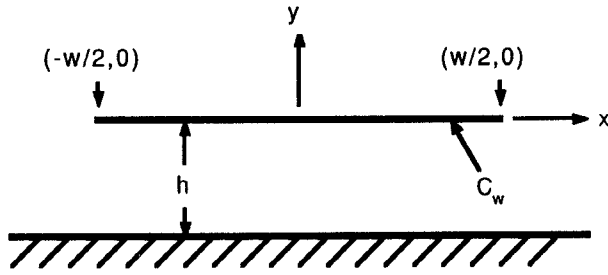

Fig. 2. Geometry of the microstrip used in the Lewin/Vainshtein current integration method.

Assuming the geometry for the microstrip as in Fig. 2, the Lorentz potential A can be expressed by the integral [9]

$$A(x,y) = \mu \oint_{C_w} G J_{s0}(\boldsymbol{\rho}') \, dl'. \tag{3}$$

An appropriate Green's function G for this microstrip configuration is

$$G(\boldsymbol{\rho}, \boldsymbol{\rho}') = \frac{1}{2\pi} \ln \left[\frac{\sqrt{(x-x')^2 + (y+2h)^2}}{\sqrt{(x-x')^2 + y^2}} \right] \tag{4}$$

where the denominator of the logarithmic function is due to the strip, and the numerator is due to its image below the ground plane. This is a purely transverse, quasi-static function. When this Green's function is used and only the longitudinal component of surface current, J_{z0}, is considered, the single Lorentz potential component A_z is

$$A_z(x,y) = \frac{\mu}{2\pi} \oint_{C_w} J_{z0}(x') \ln \left[\frac{\sqrt{(x-x')^2 + (y+2h)^2}}{\sqrt{(x-x')^2 + y^2}} \right] dl'. \tag{5}$$

The transverse variation of the magnetic field H of a quasi-TEM mode in the quasi-static limit can be expressed in terms of the Lorentz potential as [10]

$$H = \frac{1}{\mu} \nabla_T \times A \tag{6}$$

where the subscript T indicates transverse variation only, or

$\partial/\partial z = 0$. Using (6) with $A = A_z a_z$, the magnetic field in Cartesian coordinates is

$$H(x,y) = a_x \frac{1}{\mu} \frac{\partial A_z}{\partial y} - a_y \frac{1}{\mu} \frac{\partial A_z}{\partial x}. \tag{7}$$

This expression for the magnetic field can be used to find the surface currents on both sides of the infinitely thin strip by the boundary condition

$$J_{s0} = a_n \times H|_S. \tag{8}$$

Here a_n is the outward unit normal vector from the surface S, which is the surface of the strip in Fig. 2. On the top of the strip, $a_n = a_y$, $y = 0^+$, and

$$a_z J_{z0,\text{top}}(x) = a_y \times a_x \left[-H_x(x,y)|_{y=0^+} \right] \tag{9}$$

so

$$J_{z0,\text{top}}(x) = -H_x(x,y)|_{y=0^+}. \tag{10}$$

Thus only the x component of the magnetic field needs to be considered. Likewise, on the bottom of the strip, $a_n = -a_y$, $y = 0^-$,

$$a_z J_{z0,\text{bot}}(x) = -a_y \times a_x \left[H_x(x,y)|_{y=0^-} \right] \tag{11}$$

so

$$J_{z0,\text{bot}}(x) = H_x(x,y)|_{y=0^-}. \tag{12}$$

Solving for H_x from (5) and (7),

$$\begin{aligned} H_x(x,y) &= \frac{\partial}{\partial y} \left[\frac{1}{2\pi} \oint_{C_w} J_{z0}(x') \ln \left[\frac{\sqrt{(x-x')^2 + (y+2h)^2}}{\sqrt{(x-x')^2 + y^2}} \right] \right] dl' \\ &= \frac{1}{4\pi} \oint_{C_w} J_{z0}(x') \left[\frac{2(y+2h)}{(x-x')^2 + (y-2h)^2} \right. \\ &\qquad \left. - \frac{2y}{(x-x')^2 + y^2} \right] dl'. \end{aligned} \tag{13}$$

Since $J_{z0} = J_{z0,\text{top}} + J_{z0,\text{bot}}$, the current on each side of the strip can be subdivided as

$$J_{z0,\text{top}}(x) = \frac{1}{2} J_{z0}(x) - \delta J_{z0}(x) \tag{14}$$

and

$$J_{z0,\text{bot}}(x) = \frac{1}{2} J_{z0}(x) + \delta J_{z0}(x) \tag{15}$$

where

$$\begin{aligned} \delta J_{z0}(x) &= \frac{1}{2} \left(J_{z0,\text{bot}}(x) - J_{z0,\text{top}}(x) \right) \\ &= \frac{1}{2} \left[H_x(x,y)|_{y=0^-} + H_x(x,y)|_{y=0^+} \right]. \end{aligned} \tag{16}$$

If (13) is rewritten as

$$H_x(x, -y) = \frac{1}{4\pi} \oint_{C_w} J_{z0}(x') \left[\frac{2(-y+2h)}{(x-x')^2 + (-y-2h)^2} \right.$$
$$\left. - \frac{-2y}{(x-x')^2 + (-y)^2} \right] dl' \quad (17)$$

then the sum of (13) and (17) is

$$H_x(x, -y) + H_x(x, y)$$
$$= \frac{1}{8\pi} \oint_{C_w} J_{z0}(x') \left[\frac{2(y+2h)}{(x-x')^2 + (y-2h)^2} \right.$$
$$\left. + \frac{2(-y+2h)}{(x-x')^2 + (-y-2h)^2} \right] dl'. \quad (18)$$

In the limit $y \to 0^+$, half the sum (18) becomes δJ_{z0} from (16), and since J_{z0} is the total current of both sides of the strip, the contour integral for δJ_{z0} becomes the line integral

$$\delta J_{z0}(x) = \frac{h}{\pi} \int_{-w/2}^{w/2} \frac{J_{z0}(x') \, dx'}{(x-x')^2 + 4h^2}. \quad (19)$$

In terms of J_{z0} and δJ_{z0}, the integral (2) is then

$$\alpha_c = \frac{R_s}{2Z_0 I^2} \int_{-w/2+\Delta_l}^{w/2-\Delta_r} \left[\frac{1}{2} J_{z0}^2(x) + 2\delta J_{z0}^2(x) \right] dx$$
$$\approx \frac{R_s}{2Z_0 I^2} \left[\int_{-w/2+\Delta_l}^{w/2-\Delta_r} \frac{1}{2} J_{z0}^2(x) \, dx + \int_{-w/2}^{w/2} 2\delta J_{z0}^2(x) \right] dx. \quad (20)$$

The approximation is possible since $\delta J_{z0} \approx 0$ near the edges.

The integration (20) can now be done with an expression for the total current $J_{z0}(x)$ on an infinitely thin strip in a microstrip system. A closed-form expression by Kobayashi [11] is

$$\frac{J_{z0}(x)}{J_{z0}(0)} = 1 + 10 \left(1 - \frac{2x_c}{w} \right) \frac{M(x) - 1}{M(x_c) - 1} \quad (21)$$

where

$$M(x) = \frac{1}{\sqrt{1 - (2x/w)^2}} \quad (22)$$

and x_c, given by Kobayashi, is a function of the microstrip geometry w/h. Using Kobayashi's current profile, the integral (20) can be easily reduced to closed form except for the term (19), which must be approximated numerically.

In the most general case of two similar strips having the same widths but different edge shapes, the unperturbed current distribution $J_{z0}(x)$ will be the same for both. However, owing to the different edge shapes, the losses are

$$\alpha_{c1} = \frac{R_s}{2Z_0 I^2} \int_{-w/2+\Delta_{1l}}^{w/2-\Delta_{1r}} \left[J_{z0,\text{top}}^2(x) + J_{z0,\text{bot}}^2(x) \right] dx \quad (23)$$

$$\alpha_{c2} = \frac{R_s}{2Z_0 I^2} \int_{-w/2+\Delta_{2l}}^{w/2-\Delta_{2r}} \left[J_{z0,\text{top}}^2(x) + J_{z0,\text{bot}}^2(x) \right] dx \quad (24)$$

for the first and the second strip, respectively. Combining (23) and (24), the difference in attenuation constants

becomes

$$\alpha_{c2} - \alpha_{c1} = \frac{R_s}{2Z_0 I^2} \left(\int_{-w/2+\Delta_{2l}}^{-w/2+\Delta_{1l}} \left[J_{z0,\text{top}}^2(x) + J_{z0,\text{bot}}^2(x) \right] dx \right.$$
$$\left. - \int_{w/2-\Delta_{1r}}^{w/2-\Delta_{2r}} \left[J_{z0,\text{top}}^2(x) + J_{z0,\text{bot}}^2(x) \right] dx \right). \quad (25)$$

This integral, using Kobayashi's current profile, is the result used to employ the Lewin/Vainshtein current integration technique on the loss effect of different edge shapes.

B. Loss Difference Formula from a Current Model

The total current distribution J_{z0} of the strip near the left edge can be modeled as [11]

$$J_{z0}(x_l) = \frac{K_l I}{\sqrt{x_l}} + F_l(x_l) \quad (26)$$

as $x_l \to 0$, where K_l is a constant, $F_l(x_l)$ is a function of x_l which is bounded as $x_l \to 0$, and x_l is the distance from the left edge (see Fig. 1). Similarly, J_{z0} near the right edge is

$$J_{z0}(x_r) = \frac{K_r I}{\sqrt{x_r}} + F_r(x_r) \quad (27)$$

as $x_r \to 0$, where K_r, $F_r(x_r)$, and x_r are analogously defined. Since the stopping points Δ are in general very near the tip, $J_{z0,\text{top}}$ and $J_{z0,\text{bot}}$ can each be approximated as $1/2 J_{z0}$, that is, $K_l I / 2\sqrt{x_l}$ or $K_r I / 2\sqrt{x_r}$. Since $x_l = x + w/2$ and $x_r = w/2 - x$ from the geometry of Fig. 1, (25) becomes

$$\alpha_{c2} - \alpha_{c1} = \frac{R_s}{2Z_0 I^2} \left[\int_{\Delta_{2l}}^{\Delta_{1l}} \frac{2K_l^2 I^2}{4x_l} dx_l - \int_{\Delta_{1r}}^{\Delta_{2r}} \frac{2K_r^2 I^2}{4x_r} dx_r \right]$$
$$= \frac{R_s}{4Z_0} \left[K_l^2 \ln \left(\frac{\Delta_{1l}}{\Delta_{2l}} \right) + K_r^2 \ln \left(\frac{\Delta_{1r}}{\Delta_{2r}} \right) \right]. \quad (28)$$

The constants K_l and K_r, the singularity terms in the current models $J_{z0} = K_l I / \sqrt{x_l}$ and $J_{z0} = K_r I / \sqrt{x_r}$, must be determined. Of course, when J_{z0} is integrated over the entire strip, the result is the current I, but the K terms are different for each geometry and configuration. In the following, K will be related to the inductance of the zero-thickness case, so that a modified incremental inductance rule will be developed without thickness corrections. Eventually, the separate terms K_l and K_r will combine into the derivative of inductance with respect to width, $\partial L / \partial w$, so the subscripts will be dropped for brevity.

C. Relating the Singular Part of the Current to the Expanded Lorentz Potential

From (6), the quasi-static magnetic field can be expressed as

$$H = \frac{1}{\mu} \nabla_T \times A \quad (29)$$

where the potential A satisfies

$$\nabla_T^2 A_z = 0 \quad (30)$$

in the cross-sectional region surrounding the strip as in Fig. 3(a). If A_z is expanded in a sine series near the edge
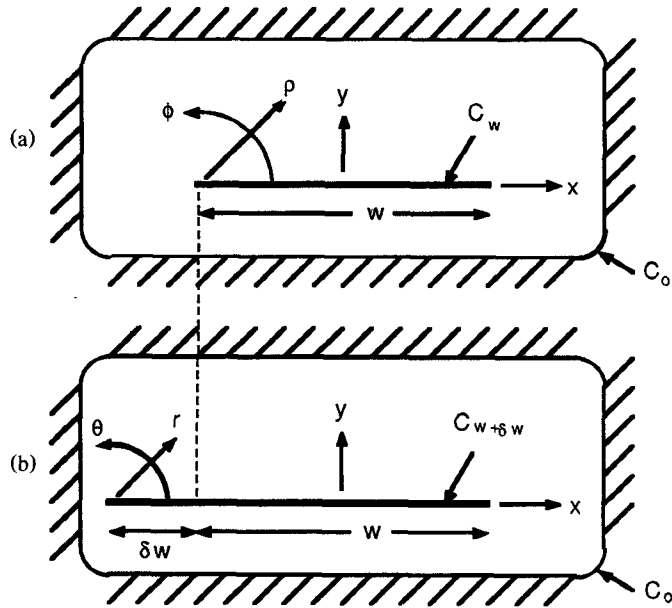
Fig. 3. (a) First case, with strip of width w and cylindrical geometry (ρ,ϕ) centered at the left edge. (b) Perturbed case having strip width $w + \delta w$ and a new cylindrical geometry (r,θ) centered at the new left edge.

$x = -w/2$ ($\rho = 0$ in Fig. 3(a)), the potential becomes

$$A_z(\rho,\phi) = A_{z0} + \sum_{m=1}^{\infty} A_{zm}(\rho)\sin\left(\frac{m\phi}{2}\right) \qquad (31)$$

where A_{z0} is the arbitrary constant value of the potential on the strip (at angles of $\phi = 0$ and 2π). In this two-dimensional, source-free environment around the edge, the scalar Laplace equation (30) becomes, upon substituting (31),

$$\left(\frac{1}{\rho}\frac{\partial}{\partial\rho}\rho\frac{\partial}{\partial\rho} - \frac{\left(\frac{m}{2}\right)^2}{\rho^2}\right)A_{zm}(\rho) = 0 \qquad (32)$$

which is solved by

$$A_{zm}(\rho) = C_m\rho^{m/2} \qquad (33)$$

where C_m is an amplitude constant. The other solution $\rho^{-m/2}$ is disallowed owing to the Meixner edge condition of finite field energy in any finite volume. From (33), (31) becomes

$$A_z(\rho,\phi) = A_{z0} + \sum_{m=1}^{\infty} C_m\rho^{m/2}\sin\left(\frac{m\phi}{2}\right). \qquad (34)$$

The transverse magnetic field components H_ϕ and H_ρ are found from (6), using only A_z. In terms of the expanded potential A_z,

$$H_\phi(\rho,\phi) = -\frac{1}{\mu}\frac{\partial A_z}{\partial\rho} = -\frac{1}{\mu}\sum_{m=1}^{\infty}\frac{m}{2}C_m\rho^{m/2-1}\sin\left(\frac{m\phi}{2}\right) \qquad (35)$$

and

$$H_\rho(\rho,\phi) = \frac{1}{\mu\rho}\frac{\partial A_z}{\partial\phi} = \frac{1}{\mu}\sum_{m=1}^{\infty}\frac{m}{2}C_m\rho^{m/2-1}\cos\left(\frac{m\phi}{2}\right). \qquad (36)$$

From the magnetic field, the surface current on both sides of the infinitely thin strip can be found from the boundary condition (8). On the top surface, the outward unit normal vector $a_n = a_\phi = a_y$, $a_\rho = a_x$, and $\phi = 0$, so

$$J_{z0,\text{top}}(\rho) = a_y \times (H_\rho a_x + H_\phi a_y)\big|_{\phi=0}$$

$$= -a_z H_\rho\big|_{\phi=0} = -\frac{1}{\mu}\sum_{m=1}^{\infty}\frac{m}{2}C_m\rho^{m/2-1}a_z. \qquad (37)$$

On the bottom surface, $a_n = -a_\phi = -a_y$, $a_\rho = a_x$, and $\phi = 2\pi$, so

$$J_{z0,\text{bot}}(\rho) = -a_y \times (H_\rho a_x + H_\phi a_y)\big|_{\phi=2\pi} = a_z H_\rho\big|_{\phi=2\pi}$$

$$= \frac{1}{\mu}\sum_{m=1}^{\infty}\frac{m}{2}C_m\rho^{m/2-1}\cos(m\pi)a_z. \qquad (38)$$

Thus, the total surface current is

$$J_{z0}(\rho) = -\frac{1}{\mu}\sum_{m=1}^{\infty}\frac{m}{2}C_m\rho^{m/2-1}(1-\cos(m\pi))$$

$$= -\frac{C_1}{\mu}\rho^{-1/2} - \frac{3C_3}{\mu}\rho^{3/2} + \cdots. \qquad (39)$$

Since on the strip surface $\rho = x_l$, (39) can be compared with the current expression from (26) to find that

$$Kl = -\frac{C_1}{\mu} \qquad (40)$$

where the l subscripts have been omitted from K and C_1. A similar derivation using the Lorentz potential expansion about the right edge yields

$$K_r l = \frac{C_{r1}}{\mu}. \qquad (41)$$

The relation (40) will be compared with another derivation based on inductances in order to eliminate C_1 and determine K in terms of an incremental inductance.

D. Relating the Singular Part of the Current with the Inductance Derivative

Fig. 3 illustrates two cases of an infinitely thin strip surrounded by a perfectly conducting surface, both invariant in the z direction. The first case has associated with it the Lorentz potential A_z, the magnetic field H, the width w, and a cylindrical geometry (ρ,ϕ) with origin at the left strip edge. The second, perturbed, case has an extra length δw to the left of the first edge, so its width is $w + \delta w$. It has a different cylindrical geometry (r,θ) centered at the new left edge, as well as quantities $A_{z\delta}$ and H_δ. In the first, the Lorentz potential expansion near the edge is (34), and in the perturbed case, it is

$$A_{z\delta}(r,\theta) = A_{z0\delta} + \sum_{m=1}^{\infty} C_{m\delta}r^{m/2}\sin\left(\frac{m\theta}{2}\right). \qquad (42)$$

The first term, $A_{z0\delta}$, the arbitrary constant potential of the strip, is set equal to A_{z0}, the potential of the first strip. The

outer perfect conductors in each case are assigned potentials of $A_z = 0$. Starting with the integral

$$\int_S B_\delta \cdot H \, dS \qquad (43)$$

where S is the enclosed area in Fig. 3(a) excluding the strip, and using the definition

$$B_\delta = \nabla_T \times A_\delta \qquad (44)$$

along with the vector identity

$$(\nabla_T \times C) \cdot D = \nabla_T \cdot (C \times D) + C \cdot (\nabla_T \times D) \qquad (45)$$

the integral becomes

$$\int_S B_\delta \cdot H \, dS = \int_S (\nabla_T \times A_\delta) \cdot H \, dS$$

$$= \int_S [\nabla_T \cdot (A_\delta \times H) + A_\delta \cdot (\nabla_T \times H)] \, dS. \qquad (46)$$

The region S has no sources, so $\nabla_T \times H = 0$ can be used to simplify the integral. Also, the divergence theorem

$$\int_S (\nabla_T \cdot F_T) \, dS = \oint_C F_T \cdot a_n \, dl \qquad (47)$$

where a_n is the outward unit normal vector, is applied. In this case, the transverse vector F_T is $(A_\delta \times H) = (A_{z0\delta} a_z \times H)$. Thus,

$$\int_S B_\delta \cdot H \, dS = \oint_C (A_\delta \times H) \cdot a_n \, dl$$

$$= \oint_{C_w + C_o} (A_{z0\delta} a_z \times H) \cdot a_n \, dl \qquad (48)$$

where C_o is the outer conductor on which $A_z = 0$ and C_w is the closed loop around the strip in Fig. 3(a). From the identity

$$A \cdot (B \times C) = C \cdot (A \times B) \qquad (49)$$

and defining a_l as the unit vector tangential to the strip contour C_w such that $a_n \times a_z = a_l$, the integral (48) reduces to

$$= \oint_{C_w} H \cdot (a_n \times A_{z0\delta} a_z) \, dl = \oint_{C_w} H \cdot (A_{z0\delta} a_l) \, dl$$

$$= \oint_{C_w} A_{z0\delta} H \cdot dl = A_{z0\delta} I \qquad (50)$$

since the contour integral

$$\oint H \cdot dl = I \qquad (51)$$

is defined as the conductor current I. From the definition of inductance, the strip potential A_{z0} can be expressed as $A_{z0} = LI$. Similarly, $A_{z0\delta} = L_\delta I_\delta$. Since the potential of the strips in both cases were set equal,

$$\int_S B_\delta \cdot H \, dS = A_{z0\delta} I = L_\delta I_\delta I = A_{z0} I = LI^2. \qquad (52)$$

Now, if the permeability μ is linear throughout,

$$\int_S B_\delta \cdot H \, dS = \int_S B \cdot H_\delta \, dS \qquad (53)$$

is true, and from a derivation similar to (43)–(50) before,

$$\int_S B \cdot H_\delta \, dS = \oint_{C_{w+\delta w}} A_z(\rho, \phi) H_\delta \cdot dl. \qquad (54)$$

Previously, the magnetic field of the first case, H, was integrated over the first width w. Now, H_δ is being integrated over the perturbed width $w + \delta w$. The difference will arise because $A_{z\delta}$ was constant, $A_{z0\delta}$, over a larger region $w + \delta w$ than what the previous integration was carried over, specifically w. In the present integral, A_z is constant, A_{z0}, over width w only and has the behavior given by the expansion in (34) beyond that. If A_z is approximated by

$$A_z(\rho, \phi) \approx A_{z0} + C_1 \sqrt{\rho} \sin\left(\frac{\phi}{2}\right) \qquad (55)$$

in the region $0 \leqslant r \leqslant \delta w$, $\theta = 0$, which is also $\delta w \geqslant \rho \geqslant 0$, $\phi = \pi$, and it is the constant A_{z0} over the remainder of the strip, then

$$\oint_{C_{w+\delta w}} A_z(\rho, \phi) H_\delta \cdot dl = \oint_{C_{w+\delta w}} A_{z0} H_\delta \cdot dl$$

$$+ 2 \int_0^{\delta w} \left[C_1 \sqrt{\rho} \sin\left(\frac{\phi}{2}\right) \right] [H_\delta \cdot d\rho]. \qquad (56)$$

Here the factor of 2 arises from integration of the top and bottom of the extra length of strip δw. Recognizing the right-hand side contour integral as the current I_δ and substituting from (36) an approximation for $H_{\rho\delta}$,

$$H_{\rho\delta}(r, \theta) \approx \frac{C_{1\delta}}{2\mu} r^{-1/2} \cos\left(\frac{\theta}{2}\right) \qquad (57)$$

the expression becomes

$$\oint_{C_{w+\delta w}} A_z(\rho, \phi) H_\delta \cdot dl \approx A_{z0} I_\delta + 2 \int_0^{\delta w} \left[C_1 \sqrt{\rho} \sin\left(\frac{\phi}{2}\right) \right]$$

$$\cdot \left[\frac{-C_{1\delta}}{2\mu} r^{-1/2} \cos\left(\frac{\theta}{2}\right) \right] d\rho. \qquad (58)$$

In the region of integration, $\phi = \pi$, $\theta = 0$, and $r = \delta w - \rho$, so

$$= A_{z0} I_\delta + 2 \int_0^{\delta w} \frac{C_1 C_{1\delta}}{2\mu} \sqrt{\frac{\rho}{\delta w - \rho}} \, d\rho$$

$$= A_{z0} I_\delta - \frac{C_1 C_{1\delta}}{\mu} \left(\frac{\pi \delta w}{2} \right) \qquad (59)$$

$$= LII_\delta - \frac{C_1 C_{1\delta} \pi \delta w}{2\mu}. \qquad (60)$$

Equating the integrals (52) and (60) by (53),

$$LII_\delta - \frac{C_1 C_{1\delta} \pi \delta w}{2\mu} = L_\delta I_\delta I \qquad (61)$$

and rearranging, the result is

$$II_\delta (L_\delta - L) = \frac{-C_1 C_{1\delta} \pi \delta w}{2\mu}. \qquad (62)$$

Taking the limiting case $\delta w \to 0$, $I_\delta \to I$, $C_{1\delta} \to C_1$, and $(L_\delta - L)/\delta w \to \partial L/\partial w$, the constant C_1 in terms of the inductance derivative is then

$$C_1^2 = \frac{-2\mu I^2 \dfrac{\partial L}{\partial w}}{\pi}. \qquad (63)$$

TABLE I
PERCENT DIFFERENCE IN FOUR DIFFERENT METHODS FOR TOTAL CONDUCTOR LOSSES
IN MICROSTRIP (INCLUDING GROUND PLANE) FROM THE PUCEL FORMULAS
$(h = 0.254 \text{ mm}, t = 18.19 \ \mu\text{m}, \epsilon_r = 1, \sigma = 4.9 \times 10^{-7} \text{ mho/m}, f = 1 \text{ GHz})$

Width (mm)	Loss Calculation Method			
	Schneider	Kaden	Spielman	Wiesbeck
0.1	22.0	−29.5	−0.9	14.3
0.2	10.9	−20.0	−3.3	9.0
0.2540	9.1	−16.9	−3.0	11.5
0.2541	18.2	−16.9	−3.0	11.5
0.3	10.5	−14.9	−2.5	8.9
0.4	7.7	−9.1	1.6	11.2
0.5	15.2	−0.5	9.5	18.7
0.5080	16.2	0.4	10.6	19.6
0.5081	4.0	−10.2	1.0	7.0
0.6	3.8	−9.9	−1.6	6.3
0.8	3.9	−9.1	−1.3	4.2
1.0	3.3	−8.4	−1.2	2.3
1.2	2.5	−7.7	−0.5	1.4
1.4	1.7	−7.2	−0.1	0.4
1.6	1.2	−6.6	0.1	0.2
1.8	0.9	−6.0	0.3	0.3

Using (40) in (63), it is found that

$$K^2 = \frac{-2\dfrac{\partial L}{\partial w}}{\mu\pi} \qquad (64)$$

which is the desired expression of K in terms of an incremental inductance. When the right edge is incremented in a similar derivation, then, using (41), the identical result (64) is obtained. Therefore,

$$K_l^2 = K_r^2 = K^2 = \frac{-2\dfrac{\partial L}{\partial w}}{\mu\pi}. \qquad (65)$$

Substituting back into (29), the final result for two general strips is

$$\alpha_{c2} = \alpha_{c1} - \frac{R_s \dfrac{\partial L}{\partial w}}{2\mu\pi Z_0}\left[\ln\left(\frac{\Delta_{1l}}{\Delta_{2l}}\right) + \ln\left(\frac{\Delta_{1r}}{\Delta_{2r}}\right)\right]. \qquad (66)$$

This amounts to a kind of incremental inductance rule analogous to Wheeler's [12] for the change in α_c caused by edge shape.

III. NUMERICAL RESULTS

A. A Survey of Microstrip Conductor Loss Methods Based on the Surface Impedance Condition

In formula (66), the attenuation factor α_{c1} is necessary as a standard, and must be accurately determined if α_{c2}, the attenuation for a strip with other edges, is to be meaningful. Various methods may be used to find α_{c1}, such as numerical computation, accurate experiment, or analytical approximations. A comparison of those methods based on the surface impedance boundary condition is done here for a rectangular-edged microstrip. Among those are the Lewin/Vainshtein current integration method of subsection II-A, using the integration stopping point of $\Delta_{rect} = t/290.8$; approximate analytical loss formulas of Pucel [3], Schneider [4], and Kaden [5]; and numerical results given by Spielman [6] and Wiesbeck [7]. Pucel's commonly accepted results are based

on Wheeler's incremental inductance rule [12], which is derived from the surface impedance condition, and on approximate closed-form expressions for the inductance of nonzero-thickness, rectangular-edged microstrips. The formulas in Pucel's paper include ground plane loss but can be altered to consider only the strip conductor. The method of Schneider [4] is similar to Pucel's in that it also is based on Wheeler's rule, and the ground plane loss contribution can be extracted. However, Schneider's formulas use different closed-formed results, in this case approximations for the microstrip characteristic impedance. Kaden [5] uses the conformal transformation technique on thin microstrips and derives loss formulas for both ground plane and strip from approximations of the resulting hyperelliptic integrals. A program for moment method solution of a general microstrip configuration with ground plane loss is given in Spielman [6] (errors exist in the program listing in [6], and were corrected by H. G. Oltman of Tecom Industries in a private communication). Another numerical method by Wiesbeck [7] implementing the moment method is used to give results with and without ground plane loss for three specific microstrip substrate heights. The results given by Finlay et al. [8] are particularly important for the case of metallization strips with thicknesses comparable to skin depth.

All of the other techniques were compared for one of the specific microstrip configurations used by Wiesbeck. Computation with these methods was done over a range of strip widths from $0.1 < w < 1.8$ mm, while all other parameters were held constant at $h = 0.254$ mm, $t = 18.19$, μm, $\epsilon_r = 1$, $\sigma = 4.9 \times 10^{-7}$ mho/m, and $f = 1$ GHz. Results of the total conductor loss including the ground plane are given in Table 1 for the methods of Pucel, Schneider, Kaden, Spielman, and Wiesbeck. Table II compares strip loss only for Pucel, Schneider, Kaden, Wiesbeck, and Lewin/Vainshtein. All entries are given in the form of a percentage difference from Pucel, p:

$$p = \frac{\alpha_{c,\text{other}} - \alpha_{c,\text{Pucel}}}{\alpha_{c,\text{Pucel}}} \times 100. \qquad (67)$$

Several observations can be made from the results. First, as the width gets narrower to 0.1 mm, the thin-strip approxi-

TABLE II
PERCENT DIFFERENCE IN FOUR DIFFERENT METHODS FOR STRIP CONDUCTOR LOSS
IN MICROSTRIP FROM THE PUCEL FORMULAS ($h = 0.254$ mm, $t = 18.19$ μm,
$\epsilon_r = 1$, $\sigma = 4.9 \times 10^{-7}$ mho/m, $f = 1$ GHz)

Width (mm)	Loss Calculation Method			
	Schneider	Kaden	Lewin	Wiesbeck
0.1	23.7	−41.5	29.4	20.4
0.2	12.0	−32.7	19.3	19.3
0.2540	10.2	−29.7	17.5	23.6
0.2541	19.3	−29.7	17.7	23.7
0.3	11.5	−27.5	15.6	22.0
0.4	8.5	−22.0	15.0	26.4
0.5	16.1	−13.9	20.6	36.7
0.5080	17.0	−13.2	21.6	37.7
0.5081	4.6	−22.4	8.6	23.1
0.6	4.5	−21.4	3.7	23.4
0.8	4.3	−19.8	−2.4	21.9
1.0	3.6	−18.3	−4.7	20.1
1.2	2.8	−17.0	−6.0	19.1
1.4	2.0	−15.8	−7.2	17.4
1.6	1.4	−14.6	−8.2	16.6
1.8	1.0	−13.7	−8.6	15.6

mation upon which each of the analytical formulas is founded starts to fail. This results in larger differences from Pucel, one of those analytical methods, at that width. Second, there is a sharp discontinuity in Pucel's loss at $w/h = 2$, or $w = 0.508$ mm. This is where the two closed-formed inductance approximations used by Pucel meet, resulting in a discontinuity of 9.0% for $t \to 0$ and slightly worse for the nonzero thickness here. Judging from the comparisons, it appears that the $w/h < 2$ approximation is at fault, giving losses which are too low. A similar discontinuity appears for Schneider at the junction of two closed-form approximations of characteristic impedance, $w/h = 1$ or $w = 0.254$ mm. The third analytical result, by Kaden, appears to be consistently lower than other results, but improves as the strip width increases. Spielman's numerical code shows excellent agreement with Pucel, but the issue of discretization error should be mentioned. In this application, the finite substrate and ground plane width was assigned a value of $l = 10w$. When this ratio was changed, conductor loss was altered significantly, especially for very large l/w ratios. Thus, discretization in numerical methods can drastically alter results. Wiesbeck also compared reasonably with Pucel in *total* loss, particularly for wider strips, but the contribution of *strip* loss varied much differently with substrate height h than Pucel. Finally, the Lewin/Vainshtein current integration method predicted higher strip loss than Pucel for narrow strips and lower strip loss for wider strips. For the following numerical comparisons, the attenuation from the Lewin/Vainshtein method, $\alpha_{c,\text{Lewin/Vainshtein}}$, will be used as α_c, keeping in mind that the ground plane loss contribution becomes more important with increasing strip width.

B. Results from the Modified Incremental Inductance Method

Formula (66) has been applied to microstrip lines of varying geometries comparing losses from the rectangular and semicircular edges (see Fig. 4), using the conductor loss α_c of the rectangular-edged strip above. The microstrip inductance for an infinitely thin strip was taken from [3], with the thickness correction terms set equal to zero. Finally, the stopping points for the two edges, $\Delta_{\text{rect}} = t/290.8$ and $\Delta_{\text{circ}} = t/124.77$, were taken from Lewin [1] and Vainshtein [2].
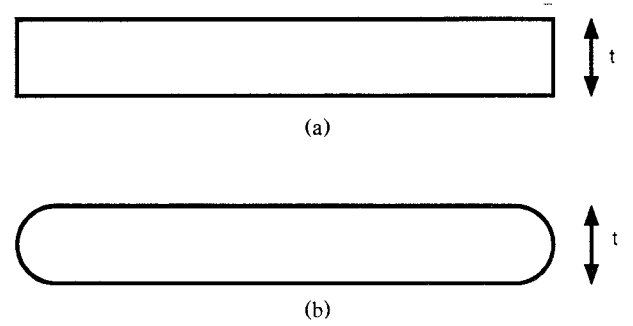

Fig. 4. (a) Rectangular-edged strip. (b) Circular-edged strip.

An approximate expression for the inductance of the microstrip is ([3])

$$L = \frac{\mu_0}{2\pi}\left[\ln\left(\frac{8h}{w}\right) + \frac{1}{32}\left(\frac{w}{h}\right)^2 + \cdots\right] \qquad (68)$$

for $w/h \leqslant 2$ and

$$L = \frac{\mu_0}{2}\left(\frac{w}{2h} + \frac{1}{\pi}\ln\left[2\pi e\left(\frac{w}{2h} + 0.94\right)\right]\right)^{-1} \qquad (69)$$

for $w/h \geqslant 2$. The required derivative $\partial L/\partial w$ is found to be

$$\frac{\partial L}{\partial w} = -\frac{\mu_0}{2\pi h}\left[\frac{h}{w} - \frac{w}{16h}\right] \qquad (70)$$

for $w/h \leqslant 2$ and

$$\frac{\partial L}{\partial w} = -\frac{\mu_0}{2\pi h}\frac{2\pi + \dfrac{1}{w/h + 1.88}}{\left(\dfrac{w}{h} + \dfrac{2}{\pi}\ln\left[2\pi e\left(\dfrac{w}{2h} + 0.94\right)\right]\right)^2} \qquad (71)$$

for $w/h \geqslant 2$.

In Fig. 5 the results of the loss comparison over a large range of strip widths and thicknesses are given. It is seen that the circular-edged microstrip produces appreciably smaller loss than the rectangular-edged lines, especially as the strip gets narrower. As expected, edge shape becomes unimpor-
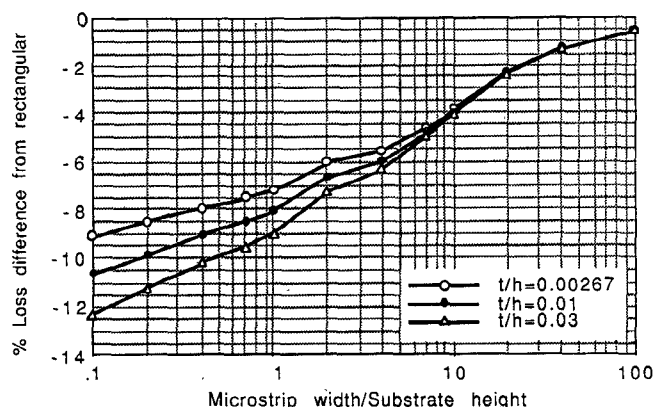
Fig. 5. Percent difference in loss between circular and rectangular edges over a wide range of microstrip widths and thicknesses using the modified incremental inductance method.
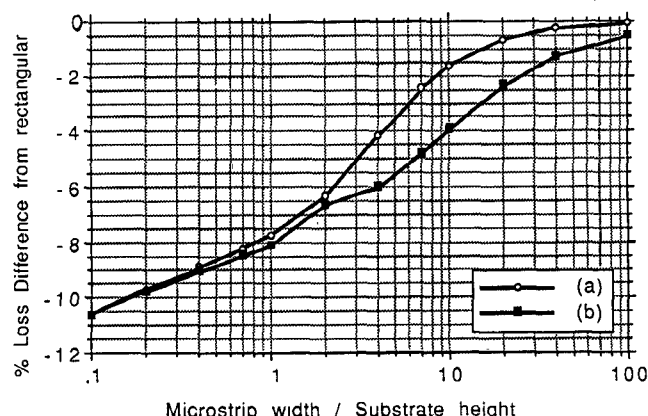

Fig. 6. Percent difference in loss between circular and rectangular edges over a wide range of microstrip widths and $t/h = 0.01$ using both (a) the perturbational loss integrals of Lewin and Vainshtein and (b) the modified incremental inductance method.

tant for very wide strips, since less of the total current is concentrated in the edges of the strip. Again, in that extreme, ground plane loss grows significantly and can no longer be ignored. Another observation is that as the strip grows thicker, the dependence on edge shape increases as well.

C. Results from the Lewin/Vainshtein Method

The effect of circular edges on loss was examined according to the modified incremental inductance method in Fig. 5. To compare the results from this method with the Lewin/Vainshtein current integration results, the current integrations were carried out to both the circular and rectangular stopping points, Δ_{circ} and Δ_{rect}, and compared. Results for a single normalized thickness, $t/h = 0.01$, are shown in Fig. 6, along with the results from (66) in Fig. 5 for the same thickness. An analysis of the results indicates that the two contrasting methods have roughly the same edge shape dependence over a wide range of strip widths.

IV. CONCLUSION AND FUTURE DIRECTIONS

The development of the result (66) was done to further the work of Lewin [1] and Vainshtein [2] with specific emphasis on the effect of different strip edge shapes on the conductor loss of planar transmission lines. A modified incremental inductance method can be used to compare loss for strips with different edges. Thus, once a result is obtained for a specific edge by other methods, as surveyed above, loss can be found for any strip edge shape if the *stopping point* Δ and the zero-thickness system inductance are known. This method holds for any planar line where quasi-TEM approximations can be used, so that the inductance is still a sensible quantity and the strip transverse current can be ignored. In an asymmetric system such as microstrip, the loss integration becomes complicated by the division of an ideal, zero-thickness current expression into the currents on the top and bottom of the strip. This method avoids that problem, although those loss integrations were developed and done here for comparison.

It has been shown that the effect of edge shape can be appreciable and should be considered. Future work might

include a more extensive list of edge shape stopping points Δ, especially for the trapezoidal edge, a common consequence of the fabrication process. An experimental verification with feasible edge shapes would be possible, especially with the trapezoidal and rectangular edges. Finally, the surface impedance boundary condition, used here and in many analyses on conductor loss, should be thoroughly examined for validity near the edge, where much of the conductor loss takes place.

REFERENCES

[1] L. Lewin, "A method of avoiding the edge current divergence in perturbation loss calculations," *IEEE Trans. Microwave Theory Tech.*, vol. MTT-32, pp. 717–719, 1984.

[2] L. A. Vainshtein and S. M. Zhurav, "Strong skin effect at the edges of metal plates," *Pis'ma Zh. Tekh. Fiz.*, vol. 12, pp. 723–729, 1986 (Engl. transl. in *Sov. Tech. Phys. Lett*, vol. 12, no. 6, pp. 298–299, 1986).

[3] R. A. Pucel, D. J. Massè, and C. P. Hartwig, "Losses in microstrip," *IEEE Trans. Microwave Theory Tech.*, vol. MTT-16, pp. 342–350, 1968. Correction in vol. MTT-16, p. 1064, 1968.

[4] M. V. Schneider, "Microstrip lines for microwave integrated circuits," *Bell Syst. Tech. J.*, vol. 48, no. 5, pp. 1421–1444, 1969.

[5] H. Kaden, "Advances in microstrip theory," *Siemens Forsch. u Entwickl. Ber.*, vol. 3, no. 2, pp. 115–124, 1974.

[6] B. E. Spielman, "Computer-aided analysis of dissipation losses in isolated and coupled transmission lines for microwave and millimeter wave integrated circuit applications," Naval Research Laboratory, Washington, DC, NRL Rep. 8009, 1976.

[7] W. Wiesbeck, "Berechnung der Dämpfung ungeschirmter Streifenleitungen," *Wiss. Ber. AEG-TELEFUNKEN*, vol. 45, no. 4, pp. 162–166, 1972.

[8] H. J. Finlay, R. H. Jansen, J. A. Jenkins, and I. G. Eddison, "Accurate characterization and modeling of transmission lines for GaAs MMIC's," *IEEE Trans. Microwave Theory Tech.*, vol. 36, pp. 961–967, 1988.

[9] R. E. Collin, *Field Theory of Guided Waves*. New York, NY: McGraw-Hill, 1960, p. 153.

[10] R. E. Collin, *Field Theory of Guided Waves*. New York: McGraw-Hill, 1960, pp. 126 ff.

[11] M. Kobayashi, "Longitudinal and transverse current distributions on microstriplines and their closed-form expression," *IEEE Trans. Microwave Theory Tech.*, vol. MTT-33, pp. 784–788, 1985.

[12] H. A. Wheeler, "Formulas for the skin effect," *Proc. IRE*, vol. 30, pp. 412–424, 1942.

Edward L. Barsotti was born in Joliet, IL, in 1966. He received the B.S. degree in 1988 from the University of Illinois, Urbana-Champaign, and the M.S. degree in 1990 from the University of Colorado, Boulder, both in electrical engineering. His thesis work concentrated on the effect of strip edge shape on microstrip conductor loss.

Since August 1990, he has been working on accelerator instrumentation at the Fermi National Accelerator Laboratory in Batavia, IL.

Faculty Fellow at the Jet Propulsion Laboratory, Pasadena, CA. In 1981–1982, he was a Visiting Professor at the Technische Hogeschool, Delft, The Netherlands. His research interests include the electromagnetic theory of wave-guiding and radiating structures at all frequencies, applied mathematics, and applied physics.

Dr. Kuester is a member of the Society for Industrial and Applied Mathematics and Commission B of the International Union of Radio Science.

✠

✠

Edward F. Kuester (S'73–M'76) was born in St. Louis, MO, on June 21, 1950. He received the B.S. degree from Michigan State University, East Lansing, in 1971, and the M.S. and Ph.D. degrees from the University of Colorado at Boulder in 1974 and 1976, respectively, all in electrical engineering.

Since 1976, he has been with the Department of Electrical Engineering at the University of Colorado, Boulder, where he is currently a Professor. In 1979, he was a Summer

John M. Dunn (S'83–M'84) received the B.A. degree in physics from Carleton College, Northfield, MN, in 1978. He then received the M.S. degree in 1980 and the Ph.D. degree from Harvard University, Cambridge, MA, in 1984, both in applied physics.

From 1984 to 1986, he was with Sandia National Laboratories as a member of the research staff. His responsibilities included the theoretical analysis of various electromagnetics problems in the areas of EMP and radar. Since the fall of 1986, he has been on the faculty at the University of Colorado, Boulder, in the Department of Electrical and Computer Engineering. His areas of interest include wave propagation problems in microwaves and optics, and CAD techniques for the design of microwave and optical circuits.